Available online at www.sciencedirect.com
ScienceDirect
Journal of Sound and Vibration 299 (2007) 656–663
JOURNAL OF SOUND AND VIBRATION
www.elsevier.com/locate/jsvi

Short Communication

Approximate step response of a nonlinear hydraulic mount using a simplified linear model

Song He, Rajendra Singh*

Acoustics and Dynamics Laboratory, Department of Mechanical Engineering and The Center for Automotive Research, The Ohio State University, Columbus, OH 43210, USA

Received 12 December 2005; received in revised form 22 May 2006; accepted 28 June 2006
Available online 29 September 2006

Abstract

A simplified dynamic stiffness type linear model is used to analytically find the step responses of a nonlinear hydraulic mount in terms of the transmitted force and top chamber pressure. The closed form solution could be efficiently implemented with effective mount parameters, and peak value and the decay curve predictions could provide some insight into the nonlinear behavior. The analytical solutions to an ideal step input correlate well with both numerical simulations (of the same linear model) and measurements when a step-like displacement excitation is applied to fixed and free decoupler mounts.

1. Introduction

Hydraulic engine mounts are designed and tuned to provide amplitude-sensitive and spectrally varying properties [1–6]; refer to Refs. [4,5] for a detailed description of the typical internal parts, their functions and basic parameters. Such mounts are usually modeled by lumping the fluid system into several control volumes as shown in Fig. 1(a). System parameters include the fluid compliances C_1 and C_2 of the top (#1) and bottom (#2) chambers, stiffness k_r and viscous damping b_r of the elastomeric rubber element (#r), fluid resistance R_i and inertance I_i of the inertia track (#i), inertance I_d and resistance R_d of the decoupler (#d). The dynamic displacement excitation $x(t)$ is applied under a mean load F_m, and the force $F_T(t)$ transmitted to the rigid base is often viewed as a measure of mount performance [1].

Typical mounts exhibit the following nonlinearities: (i) nonlinear compliances $C_1(p_1)$ and $C_2(F_m)$ due to elastomeric walls [2–5,7], (ii) vacuum formation in the top chamber during the expansion process [4,5,7], (iii) nonlinear flow resistances $R_i(q_i)$ and $R_d(q_d)$ [4,5], and (iv) the switching mechanism of the decoupler if employed [3,5,7]. Here $q_i(t)$ and $q_d(t)$ are the flow rates through the inertia track and decoupler, respectively, and $p_1(t)$ and $p_2(t)$ are dynamic pressures in the top and bottom chambers, respectively. Kim and Singh [2,3] and Tiwari et al. [4,5] have described the resulting nonlinear relationships based on laboratory experiments.

*Corresponding author. Tel.: +614 292 9044; fax: +614 292 3163.
E-mail address: singh.3@osu.edu (R. Singh).

0022-460X/$ - see front matter © 2006 Elsevier Ltd. All rights reserved.
doi:10.1016/j.jsv.2006.06.056

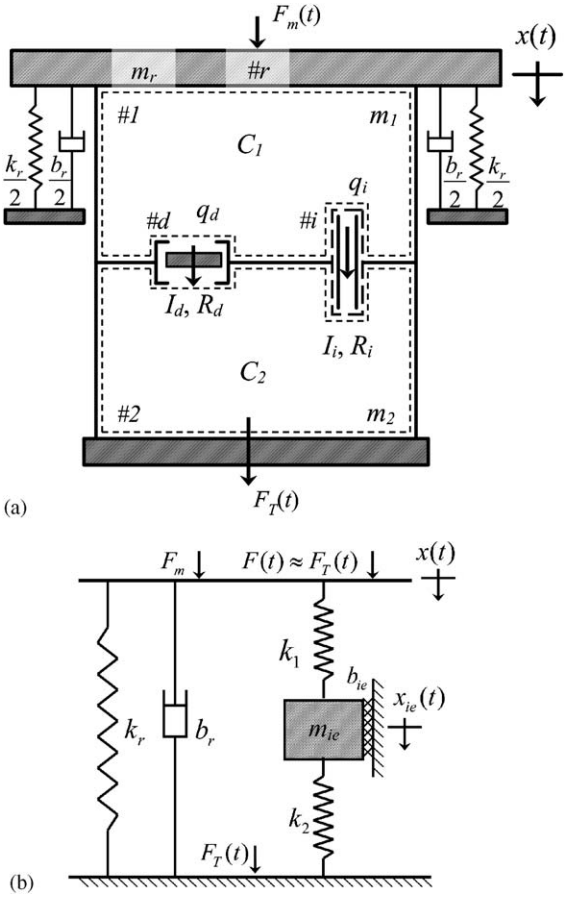

Fig. 1. Lumped models of hydraulic mount with inertia track and decoupler: (a) fluid model; and (b) analogous mechanical system.

Nonlinear continuity equations for the top and bottom chambers of Fig. 1(a) are as follows:

$$A_r\dot{x}(t) - q_i(t) - q_d(t) = C_1(p_1)\dot{p}_1(t), \tag{1}$$

$$q_i(t) + q_d(t) = C_2(F_m)\dot{p}_2(t), \tag{2}$$

where A_r is the effective piston area.

Nonlinear momentum equations for the decoupler and inertia track are derived as

$$p_1(t) - p_2(t) = I_d\dot{q}_d(t) + R_d(q_d)q_d(t), \tag{3}$$

$$p_1(t) - p_2(t) = I_i\dot{q}_i(t) + R_i(q_i)q_i(t). \tag{4}$$

The dynamic force $F_T(t)$ transmitted to the rigid base is related to the top chamber pressure and motion of the elastomeric element of Fig. 1(a) as

$$F_T(t) = k_r x(t) + b_r\dot{x}(t) + A_r p_1(t), \tag{5}$$

2. Problem formulation

The nonlinear Eqs. (1)–(5) could be linearized under certain conditions; these have been discussed in earlier papers [1,5]. Further, the authors of this communication have recently proposed a procedure that estimates the

effective system parameters based on the premise that only limited measurements of the steady state dynamic stiffness (at the frequency of excitation) are available [6]. By constructing analogous mechanical models and implementing the estimation algorithm to fixed and free decoupler mounts, linearized key parameters (such as the inertia-augmented fluid damping and decoupler gap length) could be approximated. The effects of several system nonlinearities (such as vacuum-induced asymmetric chamber compliance and damping introduced by the decoupler switching action) could also be quantified.

Let us begin with a simplified linear model of the hydraulic engine mount. Singh et al. [1] had suggested the following cross point dynamic stiffness in the Laplace (s) domain $K_{22}(s) = F_T/X(s)$ by making several simplifying assumptions. Here F_T and X are the transmitted force and displacement excitation, respectively, as shown in Fig. 1(b). One may express K_{22} for a fixed decoupler mount as follows where γ is the static stiffness, ω_{n1} and ω_{n2} (as well as ζ_1 and ζ_2) correspond to the natural frequencies (and damping ratios) of the numerator and denominator polynomials, respectively [1]. Further, Eq. (6) assumes that $b_r = 0$ and $C_2 \geqslant 100C_1$.

$$K_{22}(s) = \gamma \frac{\dfrac{s^2}{\omega_{n1}^2} + \dfrac{2\zeta_1}{\omega_{n1}}s + 1}{\dfrac{s^2}{\omega_{n2}^2} + \dfrac{2\zeta_2}{\omega_{n2}}s + 1}, \tag{6a}$$

$$\gamma = k_r + \left(\frac{A_r^2}{C_1 + C_2}\right), \quad \omega_{n1} = \sqrt{\frac{k_r}{I_i\left(A_r^2 + k_r C_1\right)}}, \quad \omega_{n2} = \sqrt{\frac{1}{I_i C_1}}, \quad \zeta_1 = \frac{1}{2}\sqrt{\frac{R_i^2\left(A_r^2 + C_1 k_r\right)}{k_r I_i}}, \quad \zeta_2 = \frac{1}{2}\sqrt{\frac{R_i^2 C_1}{I_i}}. \tag{6b–f}$$

Chief intent of this communication is to calculate an approximate analytical solution to the step input by utilizing the simplified linear model even though the hydraulic mounts exhibit significant nonlinearities [2–5,7]. In particular, note that the decoupler switching mechanism in a free decoupler device is associated with the clearance type nonlinearity that cannot be well predicted by the linear model. Therefore, only a fixed decoupler model (with $R_d \to \infty$) is considered in the analytical model. Nevertheless, the effective mount parameters of a free decoupler mount could still be utilized provided the inertia track is not completed "decoupled" from the system [6]. In such a case, an effective R_{ie} value could be used by combining R_i and R_d.

3. Analytical solutions

The transfer function of top chamber pressure $P_1(s)$ to the displacement excitation $X(s)$ is derived by using Eq. (5) and expressed in a simplified form like Eq. (6). Here, ϖ_{n1} and ξ_1 are the natural frequency and damping ratio of the numerator, as defined below:

$$\frac{P_1}{X}(s) = \frac{A_r}{C_2} \cdot \frac{I_i C_2 s^2 + R_i C_2 s + 1}{I_i C_1 s^2 + R_i C_1 s + 1} = \lambda \frac{\dfrac{s^2}{\varpi_{n1}^2} + \dfrac{2\xi_1 s}{\varpi_{n1}} + 1}{\dfrac{s^2}{\omega_{n2}^2} + \dfrac{2\zeta_2 s}{\omega_{n2}} + 1}, \tag{7a}$$

$$\lambda = \frac{A_r}{C_2}, \quad \varpi_{n1} = \sqrt{\frac{1}{I_i C_2}}, \quad \xi_1 = \frac{1}{2}\sqrt{\frac{R_i^2 C_2}{I_i}}. \tag{7b–d}$$

Here, the static gain λ implies that the static pressure is governed by the lower chamber compliance C_2 since $C_2 \geqslant 100C_1$. Define the ratios of natural frequencies and damping coefficients as $\omega_{n2}/\omega_{n1} = u$, $\zeta_2/\zeta_1 = v$, $\omega_{n2}/\varpi_{n1} = \hat{u}$ and $\zeta_2/\xi_1 = \hat{v}$. Comparison of Eqs. (6) and (7) shows that $u \cdot v = \hat{u} \cdot \hat{v} = 1$, or $\omega_{n2}\zeta_2 = \omega_{n1}\zeta_1 = \varpi_{n1}\xi_1$.

Assume zero initial conditions and apply an ideal unit step (U) displacement excitation $x(t) = U(t)$. The transmitted force in the s domain from Eq. (6) is derived as

$$F_{TS}(s) = \gamma\left[\frac{1}{s} + \left(\frac{1}{\omega_{n1}^2} - \frac{1}{\omega_{n2}^2}\right)s\Theta(s) + 2\left(\frac{\zeta_1}{\omega_{n1}} - \frac{\zeta_2}{\omega_{n2}}\right)\Theta(s)\right], \tag{8a}$$

$$\Theta(s) = \frac{\omega_{n2}^2}{(s+\zeta_2\omega_{n2})^2 + \omega_{n2}^2(1-\zeta_2^2)}. \tag{8b}$$

The step response in the time domain is derived as

$$F_{TS}(t) = \gamma\left[1 + 2\left(\frac{\zeta_1}{\omega_{n1}} - \frac{\zeta_2}{\omega_{n2}}\right)\theta(t) + \left(\frac{1}{\omega_{n1}^2} - \frac{1}{\omega_{n2}^2}\right)\theta'(t)\right], \tag{9a}$$

$$\theta(t) = \frac{\omega_{n2}}{\sqrt{1-\zeta_2^2}}\mathrm{e}^{-\sigma t}\sin\omega_d t, \quad \theta'(t) = \frac{\omega_{n2}}{\sqrt{1-\zeta_2^2}}[-\sigma\sin\omega_d t + \omega_d\cos\omega_d t]\mathrm{e}^{-\sigma t}, \tag{9b,c}$$

where $\sigma = \zeta_2\omega_{n2}$ and $\omega_d = \omega_{n2}\sqrt{1-\zeta_2^2}$. Here, $\theta(t)$ corresponds to the impulse response of a mechanical oscillator with natural frequency ω_{n2} and damping ratio ζ_2. Eq. (9a) shows that $F_{TS}(t)$ consists of three components: (i) $F_{TS1}(t) = \gamma U(t)$ is the step response of a zeroth order system when the mount acts statically as a spring of stiffness γ; (ii) $F_{TS2}(t) = 2\gamma(\zeta_1/\omega_{n1} - \zeta_2/\omega_{n2})\theta(t)$ is the impulse response of a second order system but its influence on $F_{TS}(t)$ is negligible; and (iii), $F_{TS3}(t) = \gamma(1/\omega_{n1}^2 - 1/\omega_{n2}^2)\theta'(t)$ dictates the transient response. Thus we approximate Eq. (4a) as $F_{TS}(t) \approx F_{TS1}(t) + F_{TS3}(t)$. Further, rewrite Eq. (9a) as

$$F_{TS}(t) = \gamma\left[1 + \frac{\zeta_1}{\sqrt{1-\zeta_2^2}}(u-v)\,\mathrm{e}^{-\sigma t}\sin\omega_d t + (u^2-1)\,\mathrm{e}^{-\sigma t}\cos\omega_d t\right]. \tag{10}$$

Observe that $P_1/X(s)$ shares the same denominator polynomial as $K_{22}(s)$. Since $\hat{u}\cdot\hat{v} = 1$, the top chamber pressure response given $x(t) = U(t)$ is derived as follows from Eqs. (7) and (10):

$$p_{1S}(t) = \lambda\left[1 + \frac{\xi_1}{\sqrt{1-\zeta_2^2}}(\hat{u}-\hat{v})\,\mathrm{e}^{-\sigma t}\sin\omega_d t + (\hat{u}^2-1)\,\mathrm{e}^{-\sigma t}\cos\omega_d t\right]. \tag{11}$$

From Eqs. (10) and (11), the peak $F_{TS,\max}$ and $p_{1S,\max}$ occur at $t = 0$. These values are found by assuming that $C_2 \ll C_1$ ($\gamma \approx k_r$): $F_{TS,\max} = A_r^2/C_1 + k_r = k_1 + k_r$ and $p_{1S,\max} = A_r/C_1$, where k_1 is shown in Fig. 1(b). Some design guidelines for shock control may now be formulated. For instance, a reduction in k_r may not be as efficient as decreasing A_r though both A_r and k_r remain virtually unchanged when compared with C_1. In reality, the top chamber exhibits a multi-staged nonlinearity depending on the operating conditions [3,4,7]. Further, an increase in C_1 due to the vacuum formation during the expansion process (as observed experimentally [4]) leads to flattened regions in $F_{TS,\max}$ and $p_{1S,\max}$. Thus measured peak values should be less than the theoretical result, as shown in Fig. 2.

The time instants t_p corresponding to the peak F_{TS} or p_{1S} values are derived from $\mathrm{d}F_{TS}(t)/\mathrm{d}t = 0$ and $\mathrm{d}p_{1S}(t)/\mathrm{d}t = 0$, which give identical results: $t_p(n) = n\pi/\omega_d$, $(n = 1, 2, 3\ldots)$. Consequently, t_p is governed by the damped natural frequency $\omega_d = \omega_{n2}\sqrt{1-\zeta_2^2}$ of the characteristic polynomial. Further, Eqs. (10) and (11) show that the transients decay at a exponential rate $\mathrm{e}^{-\sigma t}$. Consequently, the transient decay curves $F_{TD}(t)$ and $p_{1D}(t)$ are derived as follows:

$$F_{TD}(t) = \gamma\left(1 + \sqrt{u^4 + \left(\frac{\zeta_1^2}{1-\zeta_2^2} - 2\right)u^2 + \frac{1-2\zeta_1^2}{1-\zeta_2^2}}\,\mathrm{e}^{-\sigma t}\right), \tag{12a}$$

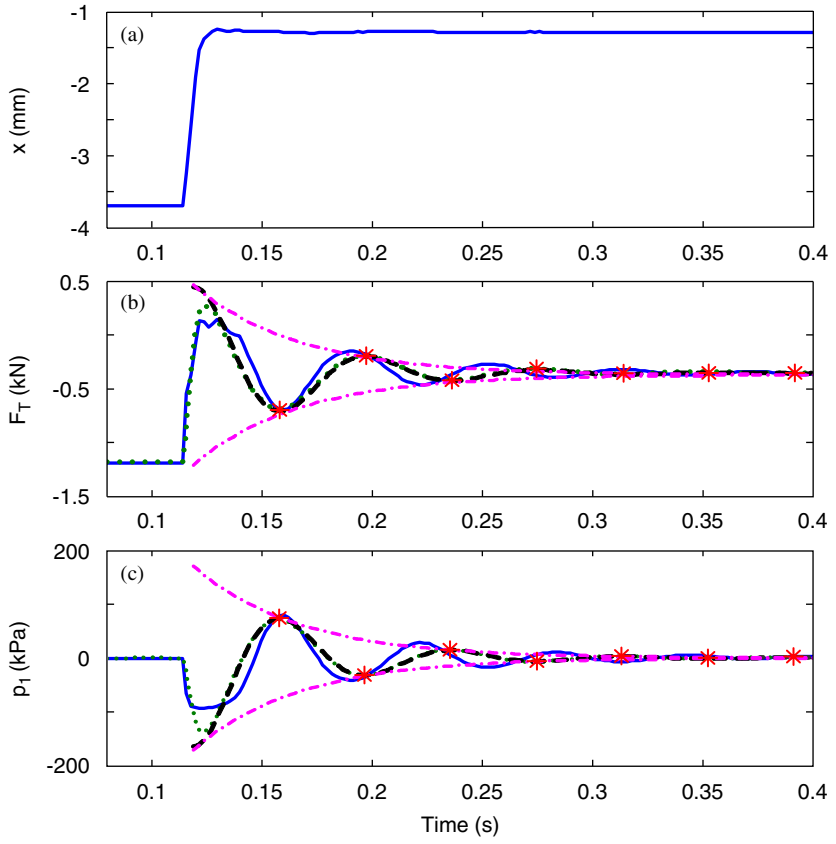

Fig. 2. Step responses of a fixed decoupler mount: (a) step-like displacement excitation $x(t) = X \cdot \hat{U}(t)$ from −3.7 to 0 mm; (b) transmitted force $F_T(t)$; (c) top chamber pressure $p_1(t)$. Key: ——— measurement; • • • • • numerical simulation of the linear model given $X \cdot \hat{U}(t)$; – – – analytical solution assuming $X \cdot U(t)$; – · – · predicted decay curve; ✱ predicted t_p values for peaks to occur based on the analytical solution.

$$p_{1D}(t) = \lambda\left(1 + \sqrt{\hat{u}^4 + \left(\frac{\xi_1^2}{1-\zeta_2^2} - 2\right)\hat{u}^2 + \frac{1-2\xi_1^2}{1-\zeta_2^2}}\,\mathrm{e}^{-\sigma t}\right). \tag{12b}$$

Since $\sigma = \zeta_2\omega_{n2} = R_i/(2I_i)$, the decay rate is essentially controlled by the inertia track or the effective damping R_{ie} [6]. The decay curves in Fig. 2 predict the transient boundaries despite some discrepancies in the first overshoot due to the vacuum nonlinearity. Next, the settling time t_{set} is defined as the time required for the transient to decay to a reasonable small value near the steady state solution $F_{TS}(\infty)$ when $t \to \infty$. Assuming an error τ as $\left|F_{TS}(t_{\text{set}}) - F_{TS}(\infty)\right| = \tau F_{TS}(\infty)$:

$$\sqrt{u^4 + \left(\frac{\zeta_1^2}{1-\zeta_2^2} - 2\right)u^2 + \frac{1-2\zeta_1^2}{1-\zeta_2^2}}\,\mathrm{e}^{-\sigma t_{\text{set}}}\left|\sin(\omega_d t_{\text{set}} + \varphi_F)\right| = \tau, \tag{13a}$$

Since $\left|\sin(\omega_d t_{\text{set}} + \varphi_F)\right| \leqslant 1$, t_{set} is dictated by the exponential term $\mathrm{e}^{-\sigma t_{\text{set}}}$ such that

$$t_{\text{set}} = \frac{1}{\sigma}\ln\frac{\sqrt{u^4 + \left(\frac{\zeta_1^2}{1-\zeta_2^2} - 2\right)u^2 + \frac{1-2\zeta_1^2}{1-\zeta_2^2}}}{\tau}. \tag{13b}$$

For the fixed decoupler mount (type D of Ref. [6]), $\sqrt{u^4+\left(\left(\zeta_1^2/\left(1-\zeta_2^2\right)\right)-2\right)u^2+\left(1-2\zeta_1^2\right)/\left(1-\zeta_2^2\right)}$, is found to be around 1.4. Thus, Eq. (13b) could be further simplified as $t_{\text{set}} \approx -(1/\sigma)\ln\tau$. Typical settling times for this mount are calculated as follows: $t_{\text{set}} = 4.6/\sigma$ given $\tau = 1\%$ and the actual error τ is 1.08%. Likewise, $t_s = 4/\sigma$ for $\tau = 2\%$ and the actual error τ is 2.4%; $t_s = 2.9/\sigma$ for $\tau = 5\%$ while the actual error τ is 5.5%.

Since the parameters of a linearized model would depend on the operating conditions, we may incorporate the empirical amplitude-sensitive parameters into the analytical predictions. For example, refer to the quasi-linear models [6] where the coefficients of Eq. (6) are estimated given the measured dynamic stiffness data. Using the mechanical analogy of Fig. 1(b) [6], Eq. (7a) is converted into the following form by assuming $k_1 \gg k_2$:

$$\frac{P_1}{X}(s) = \frac{k_1}{A_r}\frac{m_{ie}s^2 + b_{ie}s}{m_{ie}s^2 + b_{ie}s + 1}. \tag{14}$$

All effective parameters of Eq. (14) could be estimated using the quasi-linear model [6] except A_r, which could be calculated given the cross-section of the hydraulic mount. The response to $x(t) = U(t)$ is derived as

$$P_{1S}(s) = \frac{1}{A_r}\frac{\omega_{n2}^2(m_{ie}s + b_{ie})}{(s+\zeta_2\omega_{n2})^2 + \omega_{n2}^2(1-\zeta_2^2)}, \tag{15a}$$

$$\omega_{n2} = \sqrt{\frac{k_1}{m_{ie}}}, \quad \zeta_2 = \frac{b_{ie}}{2\sqrt{k_1 m_{ie}}}, \quad \sigma = \frac{b_i}{2m_i}, \quad \omega_d = \omega_{n2}\sqrt{1-\zeta_2^2}, \tag{15b–d}$$

$$p_{1S}(t) = \frac{b_{ie}}{A_r}\theta(t) + \frac{m_{ie}}{A_r}\theta'(t) = \frac{k_1}{A_r}\left(\frac{\zeta_2}{\sqrt{1-\zeta_2^2}}\sin\omega_d t + \cos\omega_d t\right)\mathrm{e}^{-\sigma t}. \tag{16}$$

Unlike Eq. (11), $p_{1S}(t)$ excludes the contribution from a zeroth order system. This implies that the predicted $p_{1S}(t)$ using the quasi-linear model converges to a steady state value of zero and thus it cannot capture the mean pressure build-up effect due to multi-staged bottom chamber compliance $C_2(F_m)$ [7]. Finally, the decay curve of dynamic top chamber pressure is derived as $p_{1D}(t) = \left(k_1/A_r\right)\left(\mathrm{e}^{-\sigma t}/\sqrt{(1-\zeta_2^2)}\right)$.

4. Results and conclusion

Two step-like displacement excitations, $x(t) = X \cdot \hat{U}(t)$, are experimentally applied by releasing the compressive preload from −3.7 mm to 0 (for the fixed decoupler mount) or to −1.32 mm (for the free decoupler mount), as shown in Fig. 2(a). Here, X is the displacement amplitude. Analytical responses assuming the ideal step input, $X \cdot U(t)$, as predicted by the K_{22} model with effective parameters from the quasi-linear model [6] are compared with both measured and numerical results given the $X \cdot \hat{U}(t)$ excitation, as shown in Figs. 2 and 3. Due to the finite rise time in $\hat{U}(t)$, slight discrepancies are observed at the initial rise time in Fig. 2. A flat region is found near the first overshoot due to the unmodeled vacuum nonlinearity during the expansion process [2,5,7]. Observe that the analytical decay curve and peak times match well with the numerical simulations of the same linear model.

Compared with the fixed decoupler mount of Fig. 2, the transients of Fig. 3 decay much faster due to the additional resistance or damping introduced by the decoupler. Two distinct regions exist beyond the first overshoot (in Fig. 3) for the free decoupler mount. One may surmise that the crossing point between the oscillatory and flat regions is when the decoupler starts to open and decouples the inertia track from the system. To better understand this phenomenon, the sequence of events is divided into five regions. Region 1: measurements coincide with linear model prediction; thus the decoupler is assumed to be closed and the system is working in the linear stiffness stage. Region 2: this corresponds to the flat regions in both $p_{1S}(t)$ and $F_{TS}(t)$ where measurements are significantly lower than the predicted values; the decoupler remains closed and vacuum occurs in the upper chamber, thereby introducing an additional compliance to C_1. Region 3: after a quick transition the decoupler is now open and it starts to move down towards the bottom stop; during this short period, the inertia track is essentially decoupled from the system and the fluid flows mainly through the

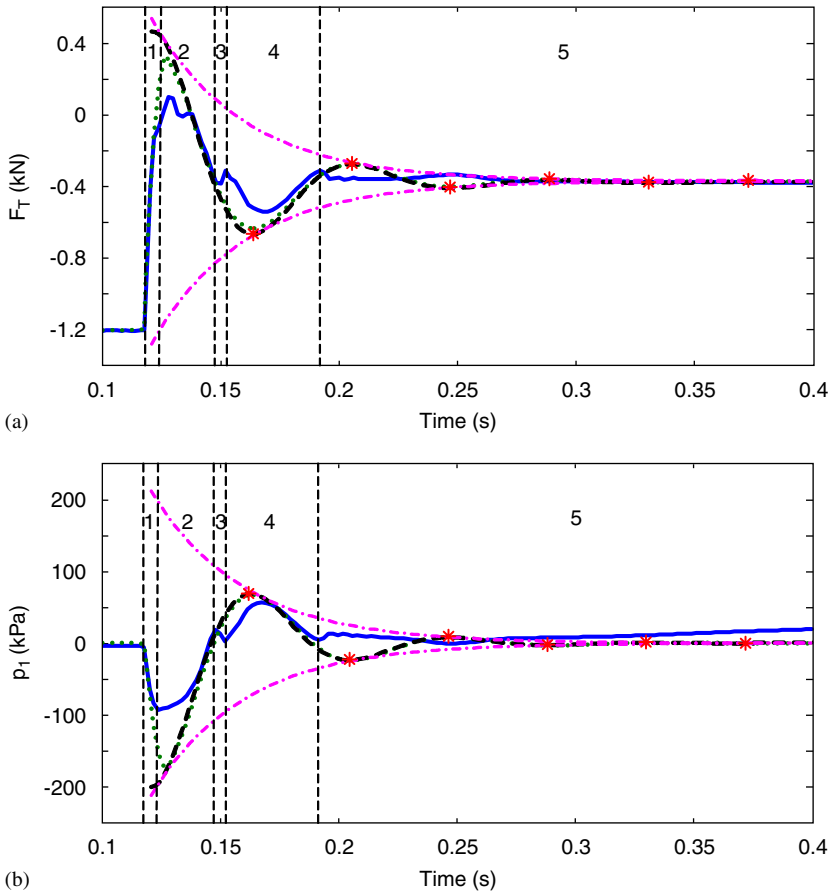

Fig. 3. Transient responses of a free decoupler mount given the $x(t) = X \cdot \hat{U}(t)$ excitation like Fig. 2(a) but from -3.7 mm to -1.32 mm: (a) transmitted force $F_T(t)$; (b) top chamber pressure $p_1(t)$. Key: ——— measurement; • • • • • numerical simulation of the linear model given $x(t) = X \cdot \hat{U}(t)$; – – – analytical solution assuming $X \cdot U(t)$; –·–·– predicted decay curve; ✳ predicted t_p values for peaks to occur based on the analytical solution.

decoupler gap to equalize the chamber pressures. Since C_2 is very high, $p_1(t)$ remains around zero and this results in a little "ripple" in the $p_1(t)$ profile. Region 4: the decoupler gap is closed and the system works in a linear manner in the decay process. Region 5: decoupler gap remains open since the transient oscillations are significantly decayed. Consequently, the "decoupled" state is dominant and transients die away quickly; this verifies that the decoupler switching mechanism can efficiently control the small amplitude excitations. The above five stages have been confirmed by employing a detailed nonlinear model that will be reported soon in an article by the same authors [7]. Overall, the simplified linear model of this article yields a reasonable prediction while providing some insight into a highly nonlinear device.

Acknowledgments

We acknowledge the experimental efforts of M. Tiwari and J. Sorenson from 1999 to 2002 (on mount D). Those studies were financially supported by the Ford Motor Company.

References

[1] R. Singh, G. Kim, P.V. Ravindra, Linear analysis of an automotive hydro-mechanical mount with emphasis on decoupler characteristics, *Journal of Sound and Vibration* 158 (2) (1992) 219–243.

[2] G. Kim, R. Singh, Non-linear analysis of automotive hydraulic engine mount, *ASME Journal of Dynamic Systems, Measurement and Control* 115 (1993) 482–487.
[3] G. Kim, R. Singh, Study of passive and adaptive hydraulic engine mount systems with emphasis on non-linear characteristics, *Journal of Sound and Vibration* 179 (1995) 427–453.
[4] M. Tiwari, H. Adiguna, R. Singh, Experimental characterization of a non-linear hydraulic engine mount, *Noise Control Engineering Journal* 51 (1) (2003) 36–49.
[5] H. Adiguna, M. Tiwari, R. Singh, Transient response of a hydraulic engine mount, *Journal of Sound and Vibration* 268 (2003) 217–248.
[6] S. He, R. Singh, Estimation of amplitude and frequency dependent parameters of hydraulic engine mount given limited dynamic stiffness measurements, *Noise Control Engineering Journal* 53 (6) (2005) 271–285.
[7] S. He, R. Singh, Discontinuous non-linearities in the hydraulic engine mount, *Journal of Sound and Vibration*, December 2005. submitted for publication.